

Krzysztof BIERNACKI\*

## ESTIMATION OF THE COEFFICIENT OF STATIC FRICTION BY MEANS OF NUMERICAL ANALYSIS

### OSZACOWANIE WARTOŚCI WSPÓŁCZYNNIKA TARCIA ZA POMOCĄ ANALIZY NUMERYCZNEJ

**Key words:**

friction coefficient, finite element method, deformations, gear pump.

**Abstract**

The friction coefficient is one of the most important tribological parameters. The value of this coefficient may be determined with the use of various methods. The friction coefficient proves to be of significance when assembling the elements of the gear pump body WPZ-80A. The bodies of these pumps consist of three elements and are manufactured in two configurations of materials. These materials are aluminium alloy AK-20 and grey iron ZL-250. Friction interaction between the elements of the pump body ensures its stable operation under load. Research so far has focused on numerical analyses for pump bodies at a set friction coefficient. This article presents a reverse analysis, i.e. an estimation of the friction coefficient value based on the WPZ-80A pump body effort. To this end, numerical analysis based on the Finite Element Method (FEM) has been used. The analysis was based on the fact that the value of friction coefficient significantly influences deformation distribution in the WPZ-80A pump body. The analysis was performed on an already constructed pump body of known geometry with no structural modifications. The value of the static friction coefficient was estimated by observing the scale of deformations in the pump body under a set load. Although the main focus was on analysing the mechanism behind the deformations, an attempt was also made at extending the application scope for FEM. Depending on the measurement method, friction coefficient values may significantly differ. Despite the differences, the values resulting from numerical analysis should not differ from the range of values obtained with other methods of analysis. The range of friction coefficient values was determined on the basis of literature studies. As a result, it was possible to verify FEM in a field different than classic effort analysis. The aim of the work presented in this article was to obtain information on tribological properties with the use of numerical analysis.

**Słowa kluczowe:**

współczynnik tarcia, metoda elementów skończonych, deformacje, pompa zębata.

**Streszczenie**

Współczynnik tarcia jest jednym z najważniejszych parametrów tribologicznych. Wartość tego współczynnika jest określana na różne sposoby. Duże znaczenie ma współczynnik tarcia dla montażu elementów zespołu korpusu pompy zębatej WPZ-80A. Korpusy tych pomp są trzyczęściowe i wykonywane są w dwóch konfiguracjach materiałowych. Jako materiały użyte zostały stop Aluminium AK-20 oraz żeliwo szare ZL-250. Wzajemne tarcie pomiędzy elementami zespołu korpusu pompy gwarantuje jej stabilną pracę pod obciążeniem. Jak do tej pory prowadzono analizy numeryczne dla korpusów pomp przy zadanym współczynniku tarcia. Postanowiono wykonać analizę odwrotną, czyli oszacować wartość współczynnika tarcia na podstawie wyciężenia zespołu korpusu pompy WPZ-80A. Cel ten postanowiono zrealizować za pomocą analizy numerycznej z użyciem metody elementów skończonych (MES). Analizę oparto na fakcie, że wartość współczynnika tarcia ma bardzo istotny wpływ na rozkład deformacji dla zespołu korpusu pompy WPZ-80A. Do analizy numerycznej przyjęto istniejący już zespół korpusu pompy o ustalonej geometrii, w którym nie wprowadzano zmian konstrukcyjnych. Wartość współczynnika tarcia oszacowywano na podstawie obserwacji wielkości deformacji dla zespołu korpusu pod zadanym obciążeniem. Oprócz tego, iż głównie skupiono się na analizie mechanizmu tych deformacji, to podjęto też próbę rozszerzenia zakresu użycia MES. Z literatury wynika, że w zależności od metody pomiaru uzyskane wartości współczynników tarcia często bardzo różnią się pomiędzy sobą. Pomimo tych różnic to wartości uzyskane z analizy numerycznej nie powinny odbiegać od zakresu wartości uzyskanych z innych metod badawczych. Dzięki temu sprawdzono MES na innym polu niż klasyczna analiza wyciężenia. Celem pracy jest zatem uzyskanie informacji na temat właściwości tribologicznych z pomocą analizy numerycznej.

\* ORCID: 0000-0001-6520-6390. Wrocław University of Science and Technology, Faculty of Mechanical Engineering, Department of Machine Design Fundamentals and Tribology, Łukasiewicza 7/9 St., 50-371 Wrocław, Poland, e-mail: krzysztof.biernacki@pwr.edu.pl.

## INTRODUCTION

Numerical analysis is typically performed with the use of the Finite Element Method (FEM) and is one of the methods employed to facilitate design processes. The method allows estimations of the values of deformations and stresses in the investigated elements and machine assemblies. It is of great significance at all design stages, such as preparing geometric sketches or potential optimizations. If FEM-based analytical models are constructed properly, the results obtained with the use of FEM are identical to the results obtained with the use of other aided design methods.

This analysis was also performed with the Finite Element Method and consisted in verifying the behaviour of pump body elements of a set and known geometry. The numerical analysis was performed on a WPZ-80A gear pump body, which was designed and manufactured in a Wrocław-based company PZL HYDRAL (currently Hamilton Sundstrand – HS Wrocław).

In this case, FEM proves very useful, as it provides answers to many questions without the need for an expensive prototyping and testing process.

Friction coefficient values can be measured with a number of known methods and experiments. Measurements performed with the use of T-05 tribological tester are described in [L. 1]. The measurements involved friction force and wear in the elements of a roll-block type friction pair. The tests were performed under technically dry friction conditions for concentrated sliding contact loaded with a force of 150 N. The mean friction coefficient values obtained under such conditions ranged for aluminium alloys between  $0.4 \leq \mu \leq 0.5$  [L. 1].

Another work [L. 2] describes friction coefficients for sealing materials. The tests were performed under dry friction conditions with the use of an inclined plane. The static friction coefficient obtained for pairs made of aluminium alloys was  $\mu = 0.28$ . The same friction coefficient for pairs made of aluminium-steel alloys was  $\mu = 0.12$  [L. 2].

Importantly, the body of the pump WPZ-80 has elements also made of aluminium alloy, more specifically of alloy AK-20. Identical materials show high friction coefficient values due to significant adhesion. Therefore, this combination is not recommended for pairs in movement [L. 3]. However, it may prove advantageous for static contact, which is the case in the assembly of the gear pump WPZ-80 body.

In such combinations, high friction force values for both aluminium and aluminium-steel alloys are confirmed in [L. 4]. The tests in [L. 4] were performed in the ball-plate system. The obtained friction coefficient values ranged between  $1.25 \leq \mu \leq 1.75$ . The value of friction coefficient  $\mu > 1$  was due to adhesion forces [L. 4].

The above demonstrates that the recorded friction coefficient values vary significantly depending on the adopted measurement method.

## DESCRIPTION OF THE GEAR PUMP BODY

Based on experiences and industrial practice, it may be concluded that a pump body optimally consists of three elements. It is a comparatively better solution in terms of the manufacturing technology, the pump body assembly, and the stress distribution. Therefore, Fig. 1 shows a schematic diagram of the pump body comprising three basic elements. The elements include a central body (1), a front console (2), and a back plate (3).

The shape of the pump WPA-80A body is similar to the shape of the pump unit, i.e. of the gear system. The design of the gear system causes the shape of the pump body to be elongated and to resemble an octagon.

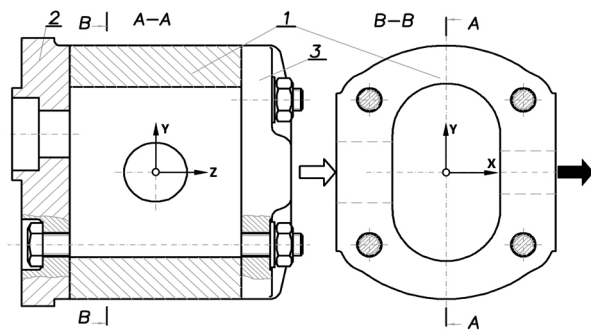


Fig. 1. Diagram of the gear pump body: 1 - central body, 2 - front console, 3 - back plate

Rys. 1. Schemat zespołu korpusu pompy zębatej: 1 - korpus centralny, 2 - konsola przednia, 3 - płyta tylna

The pumped working liquid enters the pump on the left-hand side (white arrow in the A-A cross-section, Fig. 1) and, pressurized, leaves the pump on the right-hand side (black arrow in the B-B cross-section, Fig. 1).

The elements of the pump body are connected with four bolts and their clamping force ensures the pump remains leak-tight when operating.

## PRINCIPLE OF OPERATION

The elements of the pump engage with each other on a simple principle. The front console and the back plate are mounted to the faces of the central body with bolts. The pressure between the elements is achieved by tightening four M16 bolts with a certain tightening torque  $M_d$ .

The value of the tightening torque  $M_d$  should ensure stable operation of the pump body when it is loaded with a certain working pressure  $p$ . The elements of the pump body may be said to remain in contact by friction.

An assumption was made that friction in the "friction contact points" should be simulated in the areas where the central body contacts the console and the plate and where the plate contacts bolt heads and nuts.

## CHOICE OF MATERIALS

The elements of the pump body were constructed of aluminium alloy AK-20 and grey iron ZL-250. These materials are commonly used in machine construction.

Both configurations of the pump body materials are shown in **Fig. 2** in which the aluminium alloy is indicated in blue and iron – in grey.

In the first configuration (**Fig. 2a**), all elements of the pump body are made of aluminium alloy AK-20. This solution ensures the low mass of the body of the pump WPZ-80A.

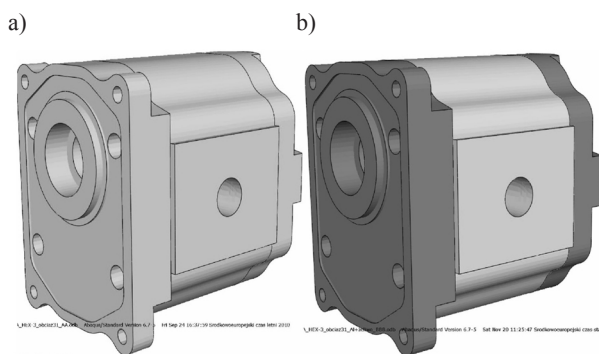


**Fig. 2. General view of the gear pump WPZ-80A body with the indicated type of material used for individual parts of the unit: a) all elements made of aluminium alloy AK-20, b) front console and back plate made of cast iron ZL-250, central body made of aluminium alloy AK-20**

Rys. 2. Widok ogólny zespołu korpusu pompy WPZ-80A z uwzględnieniem rodzaju materiału użytego na poszczególne części zespołu: a) wszystkie elementy wykonane ze stopu Aluminium AK-20, b) konsola przednia i płyta tylna wykonane są z żeliwa sferoidalnego ZL-250, korpus centralny wykonany ze stopu Aluminium AK-20

In the second configuration (**Fig. 2b**), only the central body is made of aluminium AK-20, while the front console and the back plate are made of grey iron ZL-250. Introduction of iron ZL-250, despite the increased mass, this provided two advantages:

- Lower cost (grey iron ZL-250 is cheaper than the AK-20 alloy),
- A reduced deformation of the console and of the plate by introducing a material having greater stiffness than aluminium alloy AK-20.

The materials and their strength parameters are shown in **Table 1**. The table includes the yield point  $Re$  for the AK-20 alloy and the ultimate strength  $Rr$  (stress at break) as the limit load values for the two materials. In the case of iron, the  $Rr$  value is provided, because cast iron is a brittle material and this parameter is typically accepted as the ultimate strength value.

**Table 1. Strength properties of materials used in the body of the pump WPZ-80A**

Tabela 1. Zestawienie właściwości materiałów użytych do budowy elementów korpusu pompy WPZ-80A

No.	Material	Young modulus E [MPa]	Ultimate strength [MPa]
1	Aluminium alloy AK-20	70,000	$Re^*=150$
2	Grey iron ZL-250	100,000	$Rr^{**}=250$

\* $Re$  – yield point, \*\* $Rr$  – ultimate tensile strength (stress at break)

The two material configurations required the analysis of the pump body to be performed in two versions.

## LOADS ACTING ON THE PUMP BODY

A gear pump body is subject to a complicated state of loads, which include both hydraulic and mechanical loads. These loads are due to the operation of the hydraulic machine and to the assembly of the pump body elements.

Sample loads are shown in **Fig. 3**.

Working pressure  $p$  acts on the side surfaces of the opening in the central body and on the surface of the outlet opening in this element (**Fig. 3a**). The working pressure was assumed at  $p = 20$  MPa and it is the so-called hydraulic load.

The area affected by main pressure, in which the pressure value is equal to the value of working pressure  $p = 20$  MPa, is called the high pressure area. The area can be seen in **Fig. 3a** and is indicated in red.

Also shown in the figure is the mechanical load, which is of major importance for this analysis. **Figs. 3b** and **3c** show locations where load is applied due to the tightening torque  $M_d$  for bolts pressing the front console and the back plate against the central body. The value of the tightening moment is  $M_d = 100$  Nm.

The working pressure  $p = 20$  MPa and the tightening torque  $M_d = 100$  Nm are the manufacturer's working parameters for the pump WPZ-80A.

With the known value of the tightening torque  $M_d$ , the clamping force was calculated, and it subsequently was translated into pressure, which was applied to the locations designated in red in **Figs. 3b** and **3c**.

Elements in **Fig. 3** have a number of separate areas. These areas were outlined in order to apply other loads, which have not been shown in **Fig. 3**.

The remaining loads are due to the working pressure  $p$  and the tightening torque  $M_d$ . These loads include the following, among others:

- Hydraulic load on the central body by pressure from leakages of the working liquid,

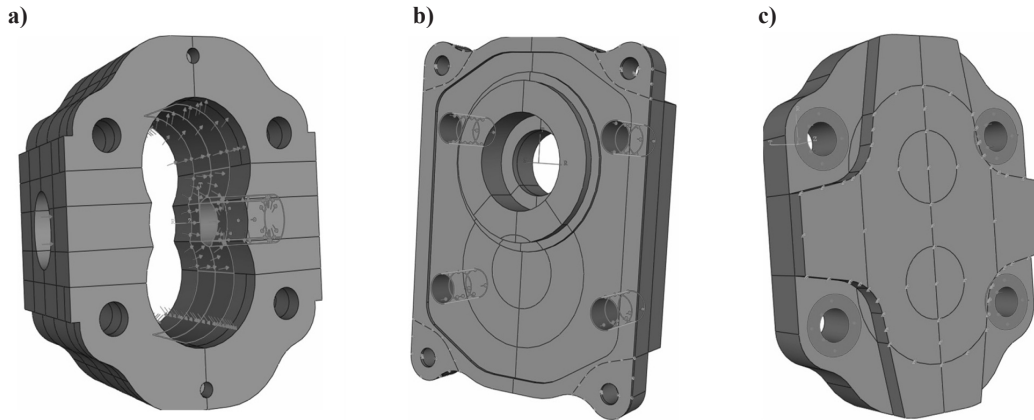


**Fig. 3. Main loads for the elements of the gear pump body: a) max. value of the working pressure  $p$  applied to the central body (No. 1, Fig. 1), b) clamping force due to the tightening of the front console (No. 2, Fig. 1), c) clamping force due to the tightening of the back plate (no. 3, Fig. 1)**

Rys. 3. Główne obciążenia dla elementów zespołu korpusu pompy zębatej: a) maksymalne ciśnienie robocze  $p$  na korpus centralny (nr 1 na Rys. 1), b) siła docisku wynikająca z dokręcenia konsoli przedniej (nr 2 na Rys. 1), c) siła docisku wynikająca z dokręcenia płyty tylnej (nr 3 na Rys. 1)

- Hydraulic load on the central body in the inlet and outlet openings due to the working liquid flowing in the X axis direction,
- Hydraulic load on the central body by the so-called increasing pressure in the increased pressure zone,
- Hydraulic load on the central body by pressure from leakages of the pumped liquid (between the body surface and the bearing housing),
- Mechanical load on the central body due to reactive forces in the bearings,
- Hydraulic load on the face of the front console from the working pressure  $p$  in the Z axis direction, and
- Hydraulic load on the face of the back plate from the working pressure  $p$  in the Z axis direction.

The values of all loads were calculated on the basis of the relationships provided in the textbook [L. 6].

These loads are not shown in Fig. 3, although they have all been included in the numerical analysis.

#### DESCRIPTION OF THE MODEL AND CHOICE OF THE CALCULATIONS SOFTWARE

The calculation model was built of 239,473 HEXA cubic elements. The elements are first order, i.e. they have 8 nodes on the corners, but they do not have nodes on the edges, as is in the case of second order elements. This type of element was selected because the model involves the “contact points” between the body, the front, and the console, as well as between the body and the back plate, and between the M16 bolt washers and the back plate. In this case, first order elements provide more accurate results and the error values may be estimated with the use of simple relationships presented in [L. 5].

**The calculations allow a conclusion that the expected error values are:  $e_u = 0.042\%$  for strain and  $e_s = 2.6\%$  for stress.**

The errors are generally expected not to exceed 5%. Therefore, the accuracy in this case seems satisfactory and the developed analytical model proves useful.

The numerical model of the gear pump WPZ-80A body was built with the use of ABAQUS version 6.14-2. This application was chosen, because it offers the most effective and complex configuration of the “contact point.” These contact points are present in the analysed gear pump on relatively large areas.

The ABAQUS application was provided by Dassault Systèmes Simulia Corp. The license No. 05UWROCLAW was provided by Wrocław Centre for Networking and Supercomputing, Wrocław University of Science and Technology.

#### METHOD AND AIM OF THE ANALYSIS

The aim of this analysis was to estimate the value of friction coefficient  $\mu$  on the basis of deformations observed in the body of the WPZ-80A gear pump.

At set load parameters, such as the working pressure  $p = 20$  MPa and the bolt tightening torque  $M_d = 100$  Nm, the values of friction coefficient  $\mu$  were changed in the “contact point.” This contact is present in the contact surfaces between the central body and the front console, as well as between the central body and the back plate.

With these assumptions, the range and value of friction coefficient  $\mu$  was selected and set when defining the contacts in the ABAQUS application. The literature [L. 1, 2, 4] allows the initial value of this coefficient to be selected for numerical analysis. Literature review suggests that the value of friction coefficient  $\mu$

should be selected from the range of  $0.28 \leq \mu \leq 1.75$ . The author believes that, in such a case, the expected value of coefficient  $\mu$  both obtained from the numerical analysis and set for the numerical analysis should not differ from the value ranges obtained with the use of other analysis methods. Therefore, the value of friction coefficient selected from the range was the first one and was  $\mu = 1.25$ . The value of  $\mu = 1.25$  was thus the initial value and served to start the numerical analysis. In each subsequent step of the analysis, the value of coefficient  $\mu$  was decreased by 0.1.

With the so-defined constant parameters  $p$  and  $M_d$ , and with variable  $\mu$ , the deformations in the body of the WPZ-80A pump were observed.

In each subsequent step of the numerical analysis, the decreasing value of friction coefficient  $\mu$  will effect an increased deformation in the model. At some point, the deformation will be sufficiently great to result in the loss of contact between the surfaces of the central body and the console and plate, respectively. The loss of contact accompanies the lowering of friction coefficient  $\mu$  despite the constant clamping force from the tightening torque  $M_d$ .

In other words, by lowering the value of coefficient  $\mu$ , limit value of this coefficient is reached, at which the contact between the elements of the body of the gear pump WPZ-80A is lost. This method was used here to identify this specific value of friction coefficient  $\mu$ .

## RESULTS OF THE NUMERICAL ANALYSIS

**Figures 4 and 5** show the numerical analysis results in the form of deformation discussion, since the deformations have a major impact on the estimated friction coefficient value. Also shown is the mechanism of contact loss between the adjacent surfaces. This loss may follow two scenarios.

In the first scenario, the load acting on the pump body not only causes the “swelling” of the central body towards the high-pressure part on the outlet side. It also entails a dislocation and a sliding action (in the direction of the OX axis, **Fig. 4b**) between the facing surfaces of the console, the plate, and the central body. As a result, the contact is lost between these surfaces. The loss of contact caused the analysis to be interrupted.

The second scenario for the loss of contact is shown in **Fig. 5**. This scenario is due to the pressure acting on the front console face and on the back plate face (in the direction of the OZ axis).

Working pressure  $p$  acts on the front console and on the back plate, causing them to deform away from the faces of the central body (in the direction of the OZ axis). As a result, both the front console and the back plate bend away from the central body. This results in the formation of gaps at the contact between the console and the central body and between the back plate and the central body. These gaps may lead to leakages. The gaps are shown in **Fig. 5** as deformations Def. 1 and Def. 2.

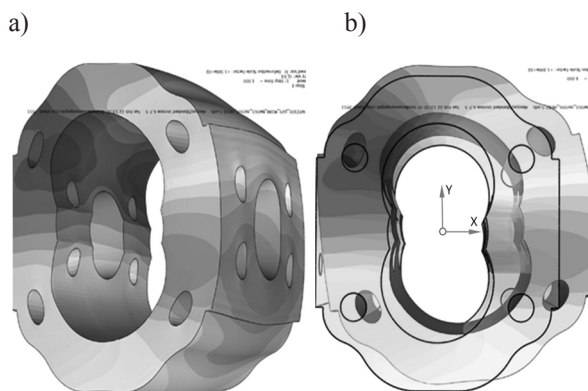


**Fig. 4. Distribution of stress on the deformed shape of the central body: a) view from the outlet side, b) view perpendicular to the face of the body**

Rys. 4. Deformacja korpusu centralnego na tle zarysu korpusu niezdeformowanego: a) widok ogólny, b) widok prostopadły do płaszczyzny czołowej

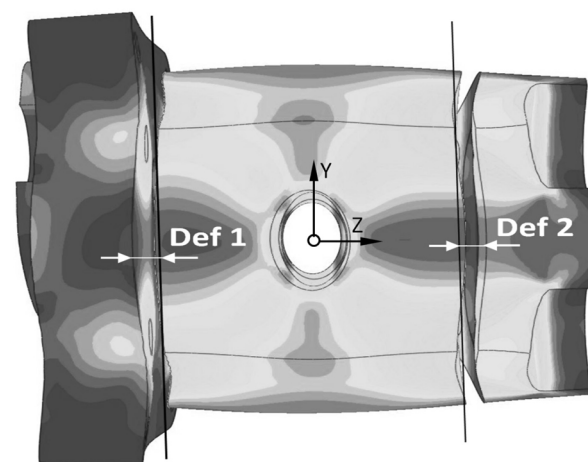


**Fig. 5. Diagram of deformations in the gear pump body**

Rys. 5. Schemat deformacji w układzie zespołu korpusu pompy zębatej

The two deformations effect a reduction in the friction surface area at the contact between the elements of the pump body. In the case of the second configuration (central body made of AK-20, the console and the back plate made of ZL-250, **Fig. 2**), the deformations will be smaller due to greater stiffness of grey iron ZL-250 as compared with aluminium AK-20.

Moreover, increasing the value of tightening torque  $M_d$  has little influence, since it does not result in increased values of deformations Def. 1 and Def. 2.

The two mechanisms cause the clamping force and the contact between the surfaces to be less intensive. The contact takes place via the value of friction coefficient  $\mu$ .

Therefore, it may be concluded that the continuous lowering of the set friction coefficient  $\mu$  values increases the potential for deformation, especially for the deformation of **Fig. 4**. At some point, the contact is lost,

as the deformation is already excessive and the friction insufficient to maintain the elements of the pump body in contact and to continue the analysis. In this case, the fact that the model lends itself to further analysis allows estimation of the value of friction coefficient  $\mu$ .

## CONCLUSIONS

The literature studies demonstrate that the values of dry friction coefficients vary and depend on for example the measurement method.

The friction coefficients obtained from the numerical analysis presented in this article provided results as follows:

In the case of material configurations of the WPZ-80A pump:

- Configuration 1 (the whole pump body made of the AK-20 alloy) – friction coefficient  $\mu = 0.55 - 0.6$ ; and,
- Configuration 2 (central body made of AK-20, the console and the plate made of iron ZL-250) – friction coefficient  $\mu = 0.5 - 0.55$ .

The values of the friction coefficients obtained in the FEM-based numerical analysis here described remain within the value ranges obtained with the use of other research methods discussed in the literature [L. 1, 2, 4].

As can be seen, the value of coefficient  $\mu$  for the pump body in the second configuration (alloy AK-20 with iron ZL-250, **Fig. 2b**) is slightly higher than for the body made completely of the aluminium AK-20 alloy (**Fig. 2a**).

This may be due to greater Young modulus  $E$  value for the iron. Grey iron ZL-250 deforms to a lesser extent than the aluminium alloy AK-20. In this case, with the assumed load, the contact surface for the iron plates will be higher than for the aluminium alloy plates. As a result, the friction coefficient value is lower for the pump body, the console, and the plate made of iron ZL-250.

The author believes that the friction coefficient values in this numerical analysis may be underrated. This may be caused by not allowing for the adhesion forces acting on large surface contact areas between the elements comprising the pump body.

Adhesion forces play a significant role in the disassembly of the pump WPZ-80. Therefore, the obtained friction coefficient  $\mu$  values are to be considered as rather minimum values for these coefficients.

FEM-based numerical analysis may thus not only allow effort analyses or other expert tests in the field of machine construction, but also offer other possibilities. One of the possibilities is to obtain approximate data on tribological factors, such as the values of friction coefficient  $\mu$ .

## REFERENCES

1. Więckowski W., Adamus J.: Badania tarciovo-zużyciowe tytanu i stopów aluminium. Inżynieria materiałowa w obróbce plastycznej. Obróbka Plastyczna Metali Vol. XXIV Nr 3 (2013). Politechnika Częstochowska 2013, pp. 169–178.
2. Wieleba W., Capanidis D., Kowalewski P., Paszkowski M.: Materiały polimerowe w uszczelnieniach – tracie statyczne. *Hydraulika i Pneumatyka* nr 6/2011. Wrocław 2011. Strony 10–13. [https://www.researchgate.net/publication/261947071\\_Materiały\\_polimerowe\\_w\\_uszczelnieniach\\_-\\_tarcie\\_statyczne](https://www.researchgate.net/publication/261947071_Materiały_polimerowe_w_uszczelnieniach_-_tarcie_statyczne)
3. Lawrowski Z.: *TRIBOLOGIA. Tarcie, zużycie i smarowanie*. Oficyna wydawnicza Politechniki Wrocławskiej, Wrocław 2008.
4. Wang L., Cai J., Zhou J., Duszczyk J.: Characteristics of the Friction Between Aluminium and Steel at Elevated Temperatures During Ball-on-Disc Tests. *Tribology Letters*. November 2009, Volume 36, Issue 2, pp. 183–190.
5. Rusiński E., Czmochoński J., Smolnicki T.: *Zaawansowana metoda elementów skończonych w konstrukcjach nośnych*. Oficyna wydawnicza Politechniki Wrocławskiej. Wrocław 2000.
6. Stryczek S.: *Napęd hydrostatyczny. Tom I, elementy*. WNT, Warszawa 1995.